Inorganic Chemistry

ARTICLE

pubs.acs.org/IC

Paramagnetic Oxotungsten(V) Complexes Containing the Hydrotris(3,5-dimethylpyrazol-1-yl)borate Ligand

Stephen Sproules,*[,†] Aston A. Eagle,[†] Michelle K. Taylor,[†,‡] Robert W. Gable,[†] Jonathan M. White,[†,§] and Charles G. Young*[,†]

[†]School of Chemistry and [§]Bio21 Molecular Science and Biotechnology Institute, University of Melbourne, Victoria 3010, Australia

Supporting Information

ABSTRACT: Sky-blue Tp*$WOCl_2$ has been synthesized from the high-yielding reaction of Tp*WO_2Cl with boron trichloride in refluxing toluene. Dark-red Tp*WOI_2 was prepared via thermal decarbonylation followed by aerial oxidation of Tp*$WI(CO)_3$ in acetonitrile. From these precursors, an extensive series of mononuclear tungstenyl complexes, Tp*WOXY [X = Cl^-, Y = OPh^-, SPh^-; X = Y = OPh^-, 2-(*n*-propyl)phenolate (PP^-), SPh^-, $SePh^-$; XY = toluene-3,4-dithiolate (tdt^{2-}), quinoxaline-2,3-dithiolate (qdt^{2-}), benzene-1,2-diselenolate (bds^{2-}); Tp* = hydrotris(3,5-dimethylpyrazol-1-yl)borate], was prepared by metathesis with the respective alkali-metal salt of X^-/XY^{2-} or $(NHEt_3)_2(qdt)$. The complexes were characterized by microanalysis, mass spectrometry, electrochemistry, IR, electron paramagnetic resonance (EPR), and electronic absorption spectroscopies, and X-ray crystallography (for X = Y = OPh^-, PP^-, SPh^-; XY = bds^{2-}). The six-coordinate, distorted-octahedral tungsten centers are coordinated by terminal oxo [W≡O = 1.689(6)−1.704(3) Å], tridentate Tp*, and monodentate or bidentate O/S/Se-donor ligands. Spin Hamiltonian parameters derived from the simulation of fluid-solution X-band EPR spectra revealed that the soft-donor S/Se ligand complexes had larger *g* values and smaller ^{183}W hyperfine coupling constants than the less covalent hard-donor O/Cl species. The former showed low-energy ligand-to-metal charge-transfer bands in the near-IR region of their electronic absorption spectra. These oxotungsten(V) complexes display lower reduction potentials than their molybdenum counterparts, underscoring the preference of tungsten for higher oxidation states. Furthermore, the protonation of the pyrazine nitrogen atoms of the qdt^{2-} ligand has been examined by spectroelectrochemistry; the product of the one-electron reduction of $[Tp^*WO(qdtH)]^+$ revealed usually intense low-energy bands.

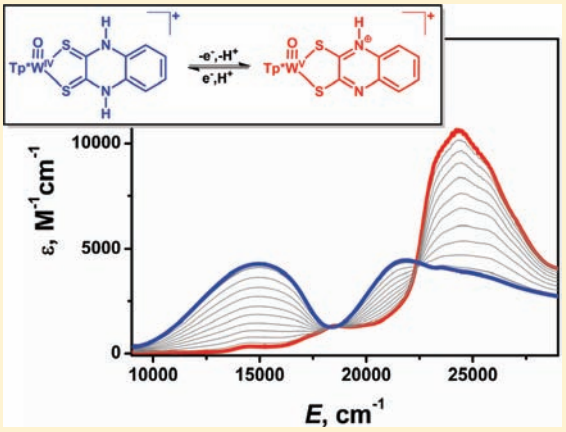

INTRODUCTION

One of the most startling biological finds of the last century was the discovery of life adjacent to deep-sea hydrothermal vents. Here, microorganisms thrive in the highly reducing, sulfur-rich environment despite the very high temperatures (>100 °C) and pressures (ca. 250 atm) associated with these extreme environments.[1] These so-called hyperthermophiles support many macroorganisms in an ecosystem devoid of sunlight. It was soon realized that these archae bacteria, perhaps the most ancient form of life on Earth,[2,3] were dependent on tungsten, and five tungsten-containing aldehyde oxidoreductases were harvested from the aptly named *Pyroccocus furiosis*.[4] Tungsten is chemically similar to its group 6 congener, molybdenum, which is an essential trace element for all forms of life.[5] The similarity of molybdenum and tungsten enzymes extends to function, active-site structure, and sequence homology, such that it was proposed that molybdenum enzymes evolved from archaeal tungsten enzymes when Earth developed an oxidizing atmosphere, thereby increasing the biological availability of molybdate in the oceans.[3,6−8] In the limited number of structurally characterized tungsten enzymes,[9] the central tungsten ion is coordinated by two pyranopterin dithiolene ligands and at least one terminal oxo ligand. Analogous pyranopterin dithiolene molybdenum enzymes exist (the dimethyl sulfoxide reductase family), and much of our thinking about the arcane tungsten enzymes is influenced by our knowledge of the better understood molybdenum enzymes; these molybdenum enzymes catalyze oxygen atom transfer or oxidative hydroxylation reactions while cycling through the IV+, V+, and VI+ oxidation states.[6,10]

High-valent oxo complexes of molybdenum and tungsten serve to mimic the biological forms of these metals in enzymes.[7,11] To that end, we have synthesized a series of bioinspired paramagnetic tungsten(V) complexes of the general formula Tp*WOXY [X = Cl^-, Y = OPh^-, SPh^-; X = Y = Cl^-, I^-, 2-(*n*-propyl)phenolate (PP^-), SPh^-, $SePh^-$; XY = toluene-3,4-dithiolate (tdt^{2-}),

Received: January 23, 2011
Published: April 15, 2011

   dx.doi.org/10.1021/ic200161m | *Inorg. Chem.* 2011, 50, 4503–4514

Scheme 1. Structures of Complexes Synthesized and Ligands Used in This Study

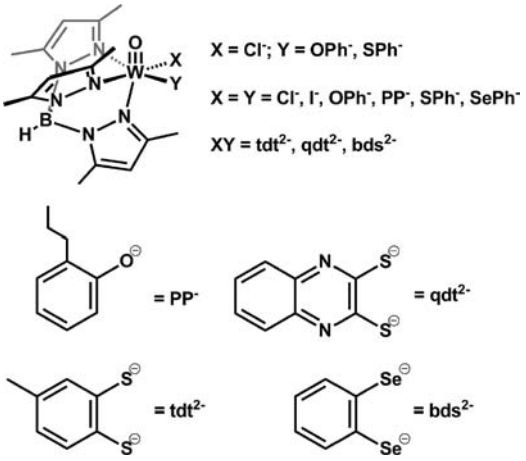

quinoxaline-2,3-dithiolate (qdt^{2-}), benzene-1,2-diselenolate (bds^{2-}); Tp* = hydrotris(3,5-dimethylpyrazol-1-yl)borate], where the XY coligands are cis to the W≡O unit (Scheme 1). These are isostructural to the Tp*MoOXY complexes prepared and studied by Enemark, Kirk, and co-workers, the electronic description of which has provided significant insights into the nature of molybdenum(V) enzyme states and the mechanisms of various molybdenum enzymes.[12−15] In particular, the complex Tp*MoO(bdt) (bdt^{2-} = 1,2-benzenedithiolate) was the first to accurately replicate the low-pH form of sulfite oxidase, with an ene-1,2-dithiolate cis to the oxo group.[15,16] Spectroscopic investigations complemented by computational studies have contributed enormously to our understanding of the electronic structure of the "MoO(dithiolene)" unit,[17−20] the salient feature of all pyranopterin-containing molybdoenzymes.

While there are numerous dioxotungsten(VI) and monoxotungsten(IV) compounds in the literature,[21] there are few mononuclear oxotungsten(V) (tungstenyl) complexes. Apart from polychloro species, $[WOCl_n]^{z-}$,[22−24] there are a handful of bis(dithiolene) complexes, e.g., $[WO(S_2C_2R_2)_2]^{-}$[25,26] and $[WO(bdt)_2]^{-}$,[27,28] and thiolate and selenolate complexes such as $[WO(EAr)_4]^{-}$ (E = S, Se; Ar = aryl)[29] and $[WO(edt)_2]^{-}$ (edt^{2-} = ethane-1,2-dithiolate).[30] Oxotungsten(V) moieties are also found in porphyrin chemistry.[31]

The synthesis of tungsten analogues to the Tp*MoOXY series has been restricted by the lack of suitable precursors. Recently, McCleverty and co-workers reported mononuclear Tp*WO(OAr)Cl and binuclear $[Tp^*WOCl]_2(\mu\text{-}OO)$ complexes, where OAr^{-} are para-substituted phenolates and OO^{2-} are para-substituted bis(phenolate) bridging ligands.[32,33] These complexes were prepared by the metathesis of Tp^*WOCl_2 under forcing conditions, to overcome the kinetic inertness of the starting material. Comparisons with the previously reported molybdenum analogues[32,34] highlighted the electrochemical and bonding changes associated with the substitution of molybdenum with its heavier group 6 congener. Herein, we detail the synthesis of an expanded series of Tp*WOXY compounds (XY = O-, S-, or Se-donor ligands) from the dihalo precursors Tp^*WOCl_2 and Tp^*WOI_2. These complexes have been examined by electronic absorption and electron paramagnetic resonance (EPR) spectroscopies and electrochemistry. Furthermore, the protonation of the dithiolene ligand in Tp*WO(qdt) has been examined by spectroelectrochemistry.

EXPERIMENTAL SECTION

Materials and Methods. The compounds Tp^*WO_2Cl,[35] $NEt_4[Tp^*W(CO)_3]$,[36,37] and $Tp^*WI(CO)_3$[37,38] were prepared by literature methods. Quinoxaline-2,3-dithiol was prepared by the method of Morrison and Furst.[39] Poly(*o*-phenylenediselenide) was synthesized following the procedure of Sandman et al.[40] All other chemicals were purchased from Aldrich Chemical Co. and used without further purification. All reactions were performed under an atmosphere of pure dinitrogen employing standard Schlenk technique, but workups, unless stated otherwise, were performed in air. Solvents were carefully dried and deoxygenated before use. Chromatographic separations and purifications were performed on 50 × 2.5 cm diameter columns using Merck Art. 7734 Keiselgel 60. IR spectra were recorded on a Biorad FTS 165 Fourier transform IR spectrophotometer as pressed KBr disks, and far-IR spectra were recorded on a Cary 17 spectrophotometer. X-band EPR spectra were recorded on a Bruker FT ECS-106 spectrometer using 1,1-diphenyl-2-picrylhydrazyl as the reference. Fluid-solution spectra were simulated using Bruker's *Simfonia*.[41] ^{1}H NMR spectra were recorded on a Varian Unity+400 spectrometer and referenced to internal $CHCl_3$ (δ_H 7.26). Electronic absorption spectra were obtained on a Perkin-Elmer Lambda 2 spectrophotometer. Mass spectra were obtained on Quattro II Micromass Triple Quad and Vacuum Generators VG ZAB 2HF mass spectrometers. Cyclic voltammograms were recorded using an Autolab PGSTAT30 interfaced with *GPES 4.9* electrochemistry software. The electrode configuration consisted of a 2 mm glassy carbon working electrode, a platinum auxiliary electrode, and a reference electrode consisting of $Ag/AgNO_3$ (0.01 M in MeCN) incorporated into a salt bridge containing a supporting electrolyte (to minimize Ag^+ leakage). Solutions of the complexes (1−2 mM) were prepared in acetonitrile/0.1 M $N^nBu_4PF_6$ or dichloromethane/0.2 M $N^nBu_4PF_6$. Potentials were referenced against internal ferrocene (Fc) and are reported relative to the saturated calomel electrode [$E_{1/2}(Fc^+/Fc)$ = 0.400 V vs SCE in acetonitrile; $E_{1/2}(Fc^+/Fc)$ = 0.460 V vs SCE in dichloromethane].[42] Electronic absorption spectra from spectroelectrochemical measurements were obtained using a Hewlett-Packard HP 8542A diode-array spectrophotometer (200−1100 nm). Elemental analyses were performed by Atlantic Microlab Inc., Norcross, GA.

Syntheses. *Tp^*WOCl_2.* A suspension of Tp^*WO_2Cl (2.00 g, 3.65 mmol) in toluene (20 mL) was treated with boron trichloride (4.00 mL of a 1.0 M *p*-xylene solution, 4.0 mmol), whereupon a suspension of orange crystals formed. The mixture was refluxed for 20 h, and a blue solid precipitated from an orange solution. The mixture was treated with ethanol (40 mL) and reduced to dryness, and then the residue was extracted with dichloromethane (120 mL) and twice filtered through a 2 cm plug of silica with dichloromethane washing. Enrichment of the blue filtrate with ethanol produced sky-blue crystals. Yield = 1.69 g (81%). Occasional traces of green Tp^*WCl_3 were removed by eluting ~300 mg of this material dissolved in CH_2Cl_2 on a silica gel chromatography column with 3:2 CH_2Cl_2/hexanes.

Anal. Calcd for $C_{15}H_{22}BN_6OCl_2W$: C, 31.72; H, 3.90; N, 14.80; Cl, 12.48. Found: C, 31.54; H, 3.85; N, 14.65; Cl, 12.68. IR (KBr, cm^{-1}): 2970 w, 2930 w, ν(BH) 2560 m, ν(CN) 1545 s, 1445 s, 1415 s, 1390 s, 1360 s, 1200 s, 1080 s, 1070 s, 1045 m, 990 w, ν(W≡O) 970 s, 880 w, 860 s, 815 s, 795 s, 690 m, 650 s, 475 w, ν(W−Cl) 340 and 320 s. Electronic spectrum (CH_2Cl_2): 15 625 (66), 28 090 (sh, ~1030), 35 340 (3740), 40 650 (7075), 43 670 cm^{-1} (6500 M^{-1} cm^{-1}). MS: m/z 567 $[M]^+$.

Tp^*WCl_3. A stirred suspension of $NEt_4[Tp^*W(CO)_3]$ (2.00 g, 2.88 mmol) in 1,2-dichloroethane (10 mL) was treated dropwise in air with thionyl chloride (0.42 mL, 5.80 mmol) and then heated to 50 °C for 5 h.

dx.doi.org/10.1021/ic200161m |*Inorg. Chem.* 2011, 50, 4503–4514

The mixture was then treated with ethanol (20 mL), and the solid product was filtered and recrystallized from dichloromethane/methanol to give green crystals. Yield = 1.50 g (89%).

Anal. Calcd for $C_{15}H_{22}BN_6Cl_3W$: C, 30.67; H, 3.78; N, 14.31; Cl, 18.11. Found: C, 30.84; H, 3.76; N, 14.11; Cl, 17.94. IR (CsI, cm^{-1}): 2930 w, 2730 w, ν(BH) 2560 m, ν(CN) 1535 s, 1445 s, 1410 s, 1385 s, 1350 s, 1260 w, 1195 s, 1065 s, 1045 m, 985 w, 970 w, 870 w, 855 m, 810 m, 795 s, 740 w, 690 m, 645 m, 595 w, 475 w, 420 w, ν(W−Cl) 335 s and 305 m. ^{1}H NMR ($CDCl_3$): δ 16.30 (s, 3 CH of Tp*), 20.69 (s, 9H, 3 CH_3 of Tp*), 21.72 (s, 9H, 3 CH_3 of Tp*). MS: m/z 588 $[M]^+$.

*Tp*WOI$_2$.* A solution of Tp*WI(CO)$_3$ (2.20 g, 3.18 mmol) in acetonitrile (20 mL) was refluxed for 3.5 h to afford a light-brown solution of Tp*WI(CO)(η-MeCN).[43] After cooling, iodine (0.80 g, 3.15 mmol) was added and the mixture was further refluxed for 1 h. The solvent was removed in vacuo, and the solids were eluted on a silica gel chromatography column using dichloromethane as the eluent. The first dark-orange band was collected, reduced to dryness, and reconstituted in tetrahydrofuran (THF; 20 mL) before being subjected to a slow stream of dioxygen gas for 1 h. The dark-red reaction mixture was left to stir overnight under an atmosphere of dioxygen. The solvent was evaporated and the residue column chromatographed using 3:2 dichloromethane/hexanes as the eluent. The red band was collected and the dark-red compound recrystallized from dichloromethane/methanol. Yield = 0.66 g (28%).

Anal. Calcd for $C_{15}H_{22}BN_6OI_2W$: C, 24.00; H, 2.95; N, 11.19. Found: C, 24.05; H, 3.03; N, 11.08. IR (KBr, cm^{-1}): 2962 w, 2927 w, ν(BH) 2561 w, ν(CN) 1544 s, 1445 s, 1414 s, 1383 w, 1354 s, 1202 s, 1070 s, 1039 w, ν(W≡O) 971 s, 856 w, 811 w, 797 w, 688 w, 646 w, 475 w. Electronic spectrum (THF): 13 200 (sh, ∼57), 15 000 (sh, ∼86), 18 800 (1870), 21 800 (sh, ∼1330), 23 200 (3100), 25 600 (2940), 28 500 (3210), 34 300 cm^{-1} (6280 M^{-1} cm^{-1}). MS: m/z 752 $[M + H]^+$.

*Tp*WO(OPh)Cl and Tp*WO(OPh)$_2$.* Elemental sodium (23 mg, 1.00 mmol) was combined with phenol (82 mg, 0.87 mmol) and refluxed in toluene (5 mL) for 40 min to afford a white suspension of NaOPh. Pale-blue Tp*WOCl$_2$ (200 mg, 0.35 mmol) was dissolved in THF (35 mL) and added to the cooled salt suspension, and the mixture was refluxed for 6 days. The solvent was evaporated and the residue column chromatographed using benzene as the eluent. The first yellow band yielded light-yellow-green crystals of Tp*WO(OPh)Cl (12 mg, 5.4%), which has been characterized elsewhere.[33] The second band was collected, yielding bright-green crystals of Tp*WO(OPh)$_2$ upon recrystallization from THF/hexanes. Yield = 51 mg (21%).

Anal. Calcd for $C_{27}H_{32}BN_6O_3W$: C, 47.46; H, 4.72; N, 12.30. Found: C, 47.54; H, 4.72; N, 12.30. IR (KBr, cm^{-1}): 2964 m, 2929 w, ν(BH) 2553 m, ν(OPh) 1588 s, ν(CN) 1542 s, 1491 s, 1481 s, 1449 s, 1417 s, 1385 m, 1367 m, 1202 m, 1074 s, ν(W≡O) 948 s, 858 s, 767 m, 754 m, 689 m, 644 w. Electronic spectrum (THF): 14 200 (46), 25 600 (970), 30 100 (sh, ∼2620), 34 100 (sh, ∼5440), 36 800 (6860), 42 000 cm^{-1} (10 350 M^{-1} cm^{-1}). MS: m/z 684 $[M + H]^+$.

*Tp*WO(PP)$_2$.* A fresh suspension of NaPP was prepared by adding sodium (32 mg, 1.39 mmol) to a toluene (30 mL) solution of 2-(*n*-propyl)phenol (1.42 mL, 1.39 mmol) and refluxing for 2 h. This suspension was treated with Tp*WOI$_2$ (500 mg, 0.67 mmol) and 18-crown-6 (5 mg), and the mixture was heated to 80−90 °C for 3 h. The solvent was removed under vacuum and the residue column chromatographed using 3:2 dichloromethane/petroleum spirits as the eluent. The first brown band was collected, and the khaki product was isolated by recrystallization from dichloromethane/methanol. Yield = 220 mg (43%).

Anal. Calcd for $C_{33}H_{44}BN_6O_3W$: C, 51.60; H, 5.73; N, 10.95. Found: C, 51.36; H, 5.65; N, 11.09. IR (KBr, cm^{-1}): 2960 w, 2924 w, ν(BH) 2548 m, ν(OPh) 1575 m, ν(CN) 1542 s, 1483 s, 1449 s, 1418 s, 1367 s, 1244 s, 1202 s, 1121 m, 1074 s, 988 w, ν(W≡O) 948 s, 870 s, 860 m, 812 m, 791 s, 753 s, 693 m, 647 s, 628 s, 473 m. MS: m/z 767 $[M]^+$.

*Tp*WO(SPh)Cl and Tp*WO(SPh)$_2$. Method 1.* A mixture of Tp*WOCl$_2$ (400 mg, 0.70 mmol) and NaSPh (200 mg, 1.51 mmol) in THF (30 mL) was refluxed for 6 days. The solvent was evaporated, and the residue was column chromatographed on silica gel using benzene as the eluent. Two bands, purple and ink blue, were collected. The overlapping portion was rechromatographed, and the respective bands were combined. Both compounds were recrystallized from THF/water, filtered, and dried in vacuo. Yields: purple Tp*WO(SPh)Cl (157 mg, 35%) and ink-blue Tp*WO(SPh)$_2$ (55 mg, 11%).

Method 2. Purple Tp*WO(SPh)Cl (150 mg, 0.23 mmol) was combined with NaSPh (60 mg, 0.45 mmol) in THF (20 mL), and the mixture was refluxed for 40 h. The solvent was removed in vacuo, and ink-blue Tp*WO(SPh)$_2$ was isolated according to the procedure outlined in method 1. Yield = 102 mg (61%).

*Tp*WO(SPh)Cl.* Anal. Calcd for $C_{21}H_{27}BN_6OSClW$: C, 39.31; H, 4.24; N, 13.10; S, 4.99. Found: C, 39.56; H, 4.70; N, 11.01; S, 4.57. IR (KBr, cm^{-1}): 2964 w, 2927 w, 2855 w, ν(BH) 2554 m, ν(SPh) 1578 m, ν(CN) 1543 s, 1475 s, 1448 s, 1415 s, 1384 m, 1359 s, 1205 s, 1074 s, 1041 s, 1025 s, ν(W≡O) 943 m, 905 w, 859 m, 812 m, 740 m, 692 m, 647 m, 473 w. Electronic spectrum (THF): 17 500 (760), 30 000 (sh, ∼4450), 31 300 (4540), 32 800 (4500), 41 200 cm^{-1} (13 490 M^{-1} cm^{-1}). MS: m/z 642 $[M + H]^+$.

*Tp*WO(SPh)$_2$.* Anal. Calcd for $C_{27}H_{32}BN_6OS_2W$: C, 45.33; H, 4.51; N, 11.75; S, 8.96. Found: C, 45.24; H, 4.56; N, 11.68; S, 8.84. IR (KBr, cm^{-1}): 2964 w, 2927 w, 2855 w, ν(BH) 2554 m, ν(SPh) 1578 m, ν(CN) 1543 s, 1475 s, 1448 s, 1415 s, 1384 m, 1359 s, 1205 s, 1074 s, 1041 s, 1025 s, ν(W≡O) 943 m, 905 w, 859 m, 812 m, 740 m, 692 m, 647 m, 473 w. Electronic spectrum (THF): 15 400 (1270), 17 900 (sh, ∼1070), 29 200 (sh, ∼6690), 32 800 (9200), 39 400 (19 170), 41 800 cm^{-1} (20 370 M^{-1} cm^{-1}). MS: m/z 716 $[M + H]^+$.

*Tp*WO(SePh)$_2$.* A yellow solution of diphenyl-1,2-diselenide (144 mg, 0.46 mmol) in THF (5 mL) was treated with 1.0 M $LiBEt_3H$ (superhydride, ∼1100 μL) until it became colorless. The solvent and volatile BEt_3 were removed in vacuo at 50 °C for 30 min. The tungsten precursor, Tp*WOCl$_2$ (200 mg, 0.35 mmol) or Tp*WOI$_2$ (200 mg, 0.27 mmol), was then added followed by THF (15 mL), whereupon the mixture was refluxed (for 2 days or 4 h, respectively). The reaction was monitored by EPR spectroscopy, and refluxing was ceased when all of the starting material had been consumed. The solvent was evaporated, and the residue was column chromatographed under anaerobic conditions using 4:1 benzene/hexanes as the eluent. An intense ink green band was collected and carefully recrystallized from a minimum volume of ice-cold THF/hexanes. The product was collected by filtration, washed with ice-cold hexanes, and dried in vacuo. Yield = 57 mg (20% based on Tp*WOCl$_2$) and 50 mg (23% based on Tp*WOI$_2$).

IR (KBr, cm^{-1}): 2960 w, 2925 m, 2852 w, ν(BH) 2553 m, ν(SePh) 1574 m, ν(CN) 1543 s, 1473 m, 1447 s, 1415 s, 1383 m, 1357 s, 1207 s, 1067 s, 1039 s, 1021 m, 957 s, ν(W≡O) 939 s, 859 m, 814 m, 786 m, 735 s, 690 s, 644 m, 466 w. Electronic spectrum (THF): 15 200 (1940), 18 200 (1990), 26 200 (sh, ∼6770), 29 700 (sh, ∼9940), 35 200 (sh, ∼22 160), 39 500 (sh, ∼29 520), 42 200 cm^{-1} (36 980 M^{-1} cm^{-1}). MS: m/z 810 $[M + H]^+$.

*Tp*WO(tdt).* A suspension of Na_2tdt was prepared by treating a solution of 3,4-toluenedithiol (100 μL, 0.75 mmol) in toluene (10 mL) with elemental sodium (59 mg, 2.57 mmol) and refluxing for 1 h. Blue Tp*WOCl$_2$ (400 mg, 0.70 mmol) was dissolved in THF (50 mL) and added to the cooled suspension via a cannula, before the mixture was refluxed for 2 days. The solvent was then removed, and the green reaction mixture was column chromatographed using benzene as the eluent. A dark-green band was collected, reduced to dryness, and recrystallized from THF/hexanes. The bright-green product was collected by filtration and dried under vacuum. Yield = 98 mg (22%).

Anal. Calcd for $C_{22}H_{28}BN_6OS_2W$: C, 40.57; H, 4.33; N, 12.90; S, 9.85. Found: C, 40.37; H, 4.24; N, 12.79; S, 9.70. IR (KBr, cm^{-1}): 2962 w,

dx.doi.org/10.1021/ic200161m |*Inorg. Chem.* 2011, 50, 4503–4514

Table 1. Crystallographic Data

	Tp*WO(OPh)$_2$	Tp*WO(PP)$_2$	Tp*WO(SPh)$_2$·1/2C$_4$H$_8$O	Tp*WO(bds)·1/2C$_6$H$_{14}$
formula	$C_{27}H_{32}BN_6O_3W$	$C_{33}H_{44}BN_6O_3W$	$C_{29}H_{36}BN_6O_{1.5}S_2W$	$C_{24}H_{33}BN_6OSe_2W$
fw	683.25	767.40	751.42	774.14
cryst size (mm^3)	0.05 × 0.05 × 0.03	0.47 × 0.47 × 0.27	0.25 × 0.20 × 0.01	0.23 × 0.21 × 0.15
cryst syst	monoclinic	monoclinic	monoclinic	monoclinic
space group	$P2_1/n$	$C2/c$	$P2_1/c$	$P2_1/c$
a (Å)	16.324(2)	30.825(5)	10.517(1)	13.067(1)
b (Å)	10.397(1)	13.277(2)	27.827(4)	14.561(1)
c (Å)	16.899(2)	17.841(4)	21.446(3)	14.521(1)
β (deg)	107.513(2)	107.00(2)	102.883(3)	99.888(1)
V (Å^3)	2735.3(5)	6983(2)	6118(1)	2721.9(4)
Z	4	8	8	4
T (K)	130(2)	293(2)	130(2)	130(2)
ρ_{calcd} (g cm^{-3})	1.659	1.460	1.632	1.889
reflns collected ($2\theta_{max}$)	14 143 (50.00)	8194 (51.96)	31 021 (50.00)	14 107 (50.00)
unique reflns [$I > 2\sigma(I)$]	4798	6837	10 773	4800
no. of param/restraints	3549/0	426/34	730/0	296/0
μ(Kα) (mm^{-1})	4.263	3.349	3.948	6.947
R_{int}	0.0571	0.0154	0.0740	0.0277
R1[a]	0.0358	0.0350	0.0632	0.0261
wR2[b] [$I > 2\sigma(I)$]	0.0505	0.0824	0.1298	0.0687
residual density (e Å^{-3})	+1.19/−0.92	+0.59/−0.80	+1.99/−2.36	+1.77/−1.51

[a] $R1 = \Sigma||F_o| - |F_c||/\Sigma|F_o|$. [b] $wR2 = \{[\Sigma w(F_o^2 - F_c^2)^2/\Sigma(w|F_o^2|)^2]\}^{1/2}$.

2927 w, 2858 w, ν(BH) 2552 m, ν(CN) 1543 s, 1450 s, 1415 s, 1386 m, 1359 s, 1201 s, 1077 s, 1062 s, 1041 m, ν(W≡O) 944 s, 857 m, 813 m, 798 m, 791 m, 691 w, 644 w, 470 w. Electronic spectrum (THF): 11 800 (200), 15 900 (120), 23 475 (sh, ∼683), 30 500 (sh, ∼4330), 34 000 (7140), 41 200, (sh, ∼26 510), 41 800 cm^{-1} (33 190 M^{-1} cm^{-1}). MS: m/z 652 [M + H]$^+$.

*Tp*WO(qdt).* A mixture of quinoxaline-2,3-dithiol (62 mg, 0.32 mmol) and triethylamine (120 μL, 0.86 mmol) in THF (10 mL) was stirred for 1 h. Red Tp*WOI$_2$ (200 mg, 0.27 mmol) was then added, and the mixture was refluxed for 15 h. The solvent was evaporated, and the residue was column chromatographed using 5:4 dichloromethane/hexanes as the eluent. The first green band was collected, reduced to dryness, and recrystallized from dichloromethane/hexanes. Yield = 42 mg (23%).

Anal. Calcd for $C_{23}H_{26}BN_8OS_2W$: C, 40.08; H, 3.80; N, 16.26; S, 9.30. Found: C, 41.18; H, 3.79; N, 15.74; S, 9.57. IR (KBr, cm^{-1}): 2927 m, ν(BH) 2557 m, ν(CN) 1544 s, 1450 s, 1415 s, 1384 m, 1357 s, 1250 m, 1218 w, 1195 s, 1169 s, 1107 s, 1074 s, 1066 s, 1043 w, ν(W≡O) 952 s, 858 m, 814 w, 795 m, 754 s, 690 w, 644 w, 596 m, 471 w. Electronic spectrum (CH_2Cl_2): 14 400 (560), 17 100 (420), 22 300 (sh, ∼3620), 24 500 (sh, ∼6140), 26 500 (17 620), 31 600 (13 970), 34 500 (16 820), 37 600 (23 860), 39 100 (26 550), 43 700 cm^{-1} (42 490 M^{-1} cm^{-1}). MS: m/z 690 [M + H]$^+$.

*Tp*WO(bds).* A 50 mL Schlenk flask was charged with poly(*o*-phenylenediselenide) (84 mg, 0.179 mmol) and THF (5 mL), and the orange suspension was treated with LiBEt$_3$H (superhydride, ∼1500 μL) until the dark-orange color had bleached to produce a faint yellow, almost colorless solution. The solvent was evaporated and the flask heated at 50 °C for 20 min under vacuum to remove volatile BEt$_3$. Red Tp*WOI$_2$ (205 mg, 0.273 mmol) was then added, followed by additional THF (10 mL), and the mixture was refluxed for 4 h. EPR spectroscopy revealed the absence of paramagnetic species in the reaction mixture (due to an excess of LiBEt$_3$H), but the tungsten(V) product formed after exposure to air for 1 h. The complex was isolated by evaporation of the solvent and anaerobic column chromatography using dry benzene as the eluent to circumvent hydrolysis of the bds^{2-} ligand. The first two bands were ignored, and an intense crimson band was collected, reduced to dryness, and recrystallized from THF/hexanes at subzero temperatures. The product was collected by filtration, washed with ice-cold hexane, and dried in vacuo. Yield = 56 mg (28%).

IR (KBr, cm^{-1}): 2954 w, 2926 w, ν(BH) 2560 m, ν(CN) 1542 s, 1445 s, 1414 s, 1382 m, 1355 s, 1220 m, 1197 s, 1075 s, 1070 s, 1048 m, 1037 m, 986 w, ν(W≡O) 950 s, 873 w, 856 m, 810 m, 788 m, 748 m, 690 m, 650 w, 643 w, 470 w. Electronic spectrum (THF): 11 100 (350), 13 400 (390), 20 200 (740), 28 400 (7220), 29 800 (7150), 33 200 (8570), 41 800 cm^{-1} (29 270 M^{-1} cm^{-1}). MS: m/z 732 [M + H]$^+$.

Crystallography. Crystal data are provided in Table 1. Crystals were coated in mineral oil and mounted on glass fibers. Diffraction-quality crystals of Tp*WO(OPh)$_2$ were grown by slow evaporation from a THF solution of the complex, while black needles of Tp*WO(SPh)$_2$ were obtained by diffusion of water into an acetonitrile solution of the compound. Brown plates of Tp*WO(bds) were obtained via diffusion of hexane into a saturated THF solution of the complex. Intensity data for Tp*WO(OPh)$_2$, Tp*WO(SPh)$_2$, and Tp*WO(bds) were collected with a Bruker SMART Apex CCD detector using Mo Kα radiation (graphite-monochromated, λ = 0.710 73). Cell parameters were acquired by the *SMART* software package, and data reduction was performed using *SAINT*. The temperature during data collection was maintained at 130 K using an Oxford Cryostream cooling device. Intensity data for Tp*WO(PP)$_2$ were collected on an Enraf-Nonius CAD4f diffractometer operating in the $\theta/2\theta$ scan mode at 293 K. The structures were solved by direct methods (*SHELXS-97*) and refined using full-matrix least-squares on F^2 (*SHELXL-97*).[44] Thermal ellipsoid plots were generated using the program *ORTEP-3*[45] integrated within the *WINGX*[46] suite of programs. All non-hydrogen atoms were included in difference maps, and anisotropic thermal parameters were employed. Hydrogen atoms were included in calculated positions. Both of the 2-(*n*-propyl)phenolate substituents for Tp*WO(PP)$_2$ were disordered and were refined using a two-site disordered model. Complex Tp*WO(bds) contained a disordered hexane solvent molecule sitting on an inversion center that could

dx.doi.org/10.1021/ic200161m |*Inorg. Chem.* 2011, 50, 4503–4514

not be satisfactorily modeled; therefore, contributions from the disordered solvent were removed by use of the *SQUEEZE* procedure.[47] All ORTEP projections have been drawn at the 50% probability level except for $Tp^*WO(PP)_2$, which is drawn at the 30% probability level to prevent the aforementioned disorder from obscuring the structure. In each case, the labeling schemes for the pyrazole rings containing N11 and N31 follow that shown for the ring containing N21. Related labeling schemes have been used for both coligands (atom numbers differ only in the first number quoted). For clarity, hydrogen atoms have been removed from all ORTEP projections.

RESULTS AND DISCUSSION

Syntheses. The title complexes were formed by metathesis reactions involving the halide precursors, Tp^*WOCl_2 and Tp^*WOI_2, and ligand salts. These reactions are quite sluggish compared to the metathesis reactions of the oxomolybdenum(V) complex, Tp^*MoOCl_2, the precursor to many oxomolybdenum(V) Tp^* complexes.[12−14,16] The kinetic inertness of Tp^*WOCl_2 versus Tp^*MoOCl_2 was also reported by Laye et al.[32] in connection with their synthesis of $Tp^*MO(biph)$ (M = Mo, W; H_2biph = 2,2′-biphenol). The synthesis of the title compounds has been facilitated by the development of an improved synthesis for Tp^*WOCl_2 and the synthesis of Tp^*WOI_2, which undergoes more facile halide substitution reactions. Characterization data for these two compounds are presented here for the first time.

The new preparation for Tp^*WOCl_2 begins with the addition of BCl_3 to a suspension of Tp^*WO_2Cl in toluene, which results in the precipitation of an orange, moisture-sensitive compound that is probably an oxoborane acid−base adduct of the type $Tp^*WO(O\cdot BCl_3)Cl$.[48] Prolonged reflux of the reaction mixture converts this compound to blue Tp^*WOCl_2 in high yield, with bright-green Tp^*WCl_3 as a minor product; the latter compound was briefly described by Millar et al.[49] An alternative synthesis for Tp^*WCl_3, developed here, involves the addition of $SOCl_2$ to a yellow suspension of $NEt_4[Tp^*W(CO)_3]$ in 1,2-dichloroethane, followed by heating at 50 °C to ensure complete reaction, and recrystallization of the precipitated product from CH_2Cl_2/MeOH. Both Tp^*WOCl_2 and Tp^*WCl_3 are indefinitely air-stable as crystalline solids or in solution. These complexes are soluble in chlorinated solvents, slightly soluble in aromatic solvents, and insoluble in hydrocarbons and alcohols.

Dark-red Tp^*WOI_2 was synthesized in a multistep sequence involving (i) oxidation of yellow $NEt_4[Tp^*W(CO)_3]$ by iodine to generate dark-brown $Tp^*WI(CO)_3$, (ii) thermal decarbonylation of $Tp^*WI(CO)_3$ in acetonitrile to give light-brown $Tp^*W(CO)I(\eta^2\text{-MeCN})$, (iii) treatment of $Tp^*W(CO)I(\eta^2\text{-MeCN})$ with iodine to yield orange $Tp^*WI_2(CO)$, and (iv) autoxidation of $Tp^*WI_2(CO)$ to form dark-red Tp^*WOI_2. The final product was isolated by column chromatography using 3:2 dichloromethane/hexanes as the eluent in a modest overall yield of 28%. The complex can also be prepared by the reaction of $Tp^*WOI(CO)$[50] with iodine. The complex is soluble in chlorinated solvents (with slow conversion to Tp^*WOCl_2), THF, acetonitrile, and aromatic hydrocarbons. It is insoluble in hydrocarbons and alcohols.

The halo precursors above react with alkali-metal salts such as NaOPh, NaPP, NaSPh, LiSePh, Na_2tdt, and Li_2bds and the ammonium salt $(NEt_3H)_2(qdt)$ to produce derivatives of the type Tp^*WOXY (Scheme 1). The products from reactions with Na_2edt (edt^{2-} = 1,2-ethanedithiolate), $Na_2(edtMe_2)$ ($edtMe_2^{2-}$ = 2,3-butanedithiolate), and Na_2cat (cat^{2-} = catecholate) were highly unstable and were only detected by EPR in situ. The course of the reactions was conveniently monitored by EPR spectroscopy. The reaction times varied according to the hardness of the introduced donor ligand, with longer reaction times required for O- versus S/Se-donor ligands.

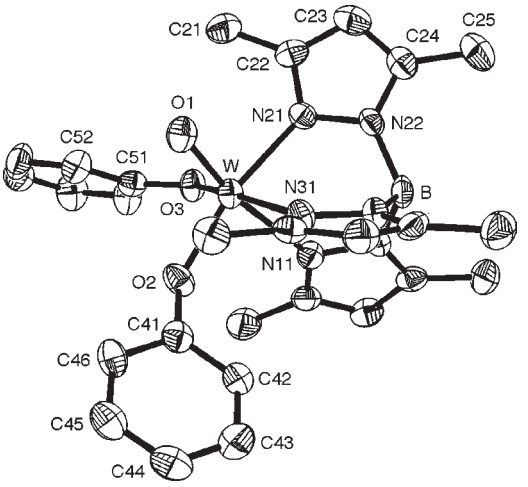

Figure 1. ORTEP projection and partial labeling scheme for $Tp^*WO(OPh)_2$.

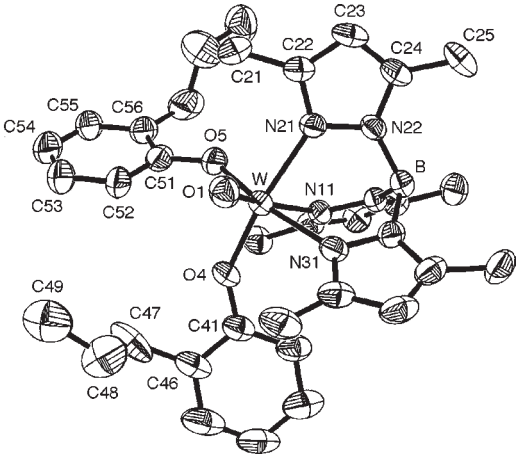

Figure 2. ORTEP projection and partial labeling scheme for $Tp^*WO(PP)_2$.

All Tp^*WOXY complexes, with the exception of $Tp^*WO(SePh)_2$ and $Tp^*WO(bds)$, are indefinitely air-stable as solids. The aforementioned complexes are moisture-sensitive, with the co-ligands readily displaced by hydroxide. Soft S- and Se-donor ligand complexes are unstable in solution, their color fading with concomitant precipitation of a white solid over a few days; they are also unstable in chlorinated solvents, reverting to Tp^*WOCl_2. With the exception of $Tp^*WO(qdt)$, all are soluble in THF and aromatic solvents and less soluble in acetonitrile. Mint-green $Tp^*WO(qdt)$ is sparingly soluble in all but chlorinated solvents. Generally, the compounds are insoluble in aliphatic hydrocarbons and alcohols. However, purple $Tp^*WO(SPh)Cl$ and ink-blue $Tp^*WO(SPh)_2$ are remarkably soluble in all of the aforementioned solvents but are insoluble in water.

The complexes have been characterized by a wide variety of techniques, although sensitivity and thermal instability prevented the

dx.doi.org/10.1021/ic200161m |*Inorg. Chem.* 2011, 50, 4503–4514

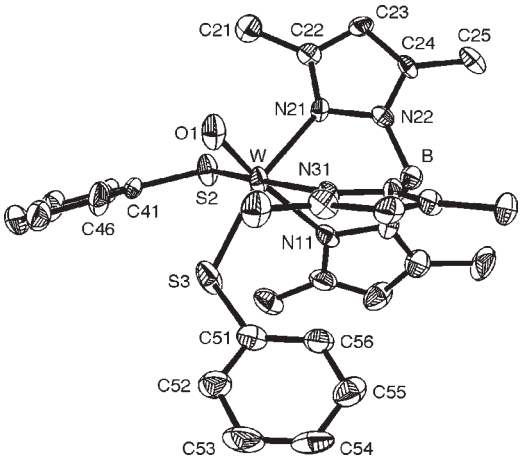

Figure 3. ORTEP projection and partial labeling scheme for $Tp^*WO(SPh)_2$.

Table 2. Selected Bond Distances (Å) and Angles (deg) for Tp^*WOX_2 Complexes[a]

	$Tp^*WO(OPh)_2$	$Tp^*WO(PP)_2$	$Tp^*WO(SPh)_2$[b]
W−O1	1.704(3)	1.695(4)	1.698(7), 1.689(6)
W−E2	1.936(3)	1.950(3)	2.389(2), 2.392(2)
W−E3	1.946(3)	1.942(3)	2.380(3), 2.379(2)
W−N11	2.309(4)	2.300(4)	2.325(8), 2.331(7)
W−N21	2.146(4)	2.149(4)	2.159(7), 2.176(7)
W−N31	2.145(4)	2.161(4)	2.172(7), 2.150(7)
O1−W−E2	103.5(2)	102.3(2)	98.7(2), 99.4(2)
O1−W−E3	101.9(2)	102.7(2)	100.3(2), 100.9(2)
O1−W−N11	168.5(2)	169.6(2)	172.2(3), 171.8(3)
O1−W−N21	90.7(2)	91.9(2)	94.5(3), 92.9(3)
O1−W−N31	92.3(2)	91.5(2)	91.7(3), 96.0(3)
E2−W−E3	87.5(1)	89.6(2)	91.03(9), 91.75(9)
E2−W−N11	86.5(2)	85.3(2)	86.72(18), 81.17(18)
E2−W−N21	165.8(2)	165.8(2)	89.63(18), 87.6(2)
E2−W−N31	94.3(1)	93.4(2)	167.5(2), 162.9(2)
E3−W−N11	84.1(1)	84.3(2)	85.2(2), 87.26(18)
E3−W−N21	89.6(1)	88.4(2)	164.9(2), 166.1(2)
E3−W−N31	164.9(2)	164.5(2)	93.89(19), 92.5(2)
N11−W−N21	79.4(2)	80.5(2)	79.8(3), 78.9(3)
N11−W−N31	81.0(2)	80.8(2)	82.3(3), 82.5(3)
N21−W−N31	85.0(2)	85.0(2)	82.7(2), 84.4(3)
W−E2−C41	135.4(3)	142.0(5)	116.4(3), 113.7(3)
W−E3−C51	135.5(3)	136.4(5)	113.0(3), 116.0(3)

[a] In the parameter list, E refers to the donor atom of the monodentate coligand: For $Tp^*WO(OPh)_2$, E = O; for $Tp^*WO(PP)_2$, E2 = O4 and E3 = O5; for $Tp^*WO(SPh)_2$, E = S. [b] Parameters for molecules 1 and 2, respectively (atom numbers refer to molecule 1, with corresponding parameters for molecule 2 given).

collection of some microanalytical data. In all cases, an $[M + H]^+$ peak cluster was observed by mass spectrometry. IR spectra exhibited a single, strong ν(W≡O) band in the range 971−939 cm^{-1}, in the region of other mono- and dinuclear tungstenyl complexes.[22,24,29,32,33] Characteristic ligand bands were observed for Tp* [ν(BH) 2561−2548 cm^{-1} and ν(CN) 1545−1542 cm^{-1}] and the aromatic C−C mode in O-, S-, and Se(E)-donor monodentate coligands [ν(EPh) 1592−1574 cm^{-1}]. Symmetric and antisymmetric WCl_2 stretches were observed for Tp^*WOCl_2 at 340 and 320 cm^{-1} and Tp^*WCl_3 at 335 and 305 cm^{-1}, respectively.

Table 3. Selected Bond Distances (Å) and Angles (deg) in $Tp^*WO(bds)$

W−O1	1.704(3)	W−Se2	2.5143(5)	W−Se3	2.5038(5)
W−N11	2.369(3)	W−N21	2.156(3)	W−N31	2.155(3)
Se2−C2	1.920(4)	Se3−C3	1.915(4)	C2−C3	1.388(5)
O1−W−Se2	100.1(1)	O1−W−Se3	99.1(1)	O1−W−N11	171.1(1)
O1−W−N21	91.75(1)	O1−W−N31	94.2(1)	Se2−W−Se3	86.70(1)
Se2−W−N11	87.77(8)	Se2−W−N21	93.05(8)	Se2−W−N31	168.03(9)
Se3−W−N11	85.40(7)	Se3−W−N21	166.54(9)	Se3−W−N31	93.37(8)
N11−W−N21	80.3(1)	N11−W−N31	81.1(1)	N21−W−N31	84.1(1)
W−Se2−C2	100.9(1)	W−Se3−C3	101.0(1)	Se2−C2−C3	122.1(3)
Se3−C3−C2	122.6(3)				

Crystal Structures. The crystal structures of $Tp^*WO(OPh)_2$ (Figure 1), $Tp^*WO(PP)_2$ (Figure 2), and $Tp^*WO(SPh)_2 \cdot {}^1/_2C_4H_8O$ (Figure 3) have been determined by X-ray crystallography; selected bond distances and angles are summarized in Table 2. In all three structures, tungsten is found in a distorted octahedral coordination sphere comprised of the three facially bound nitrogen atoms of the Tp* ligand, one terminal oxo ligand, and two monodentate ligands (X = OPh^-, PP^-, and SPh^-). The structures of $Tp^*WO(OPh)_2$ and $Tp^*WO(PP)_2$ (parameters in brackets) are almost identical with that of $Tp^*MoO(OPh)_2$.[51] The short W−O1 distances of 1.704(3) [1.695(4) Å] are typical of a terminal, multiply bonded oxo ligand on tungsten.[28,32,33] The W−O2 and W−O3 distances of 1.936(3) and 1.946(3) Å [W−O4 = 1.950(3) Å and W−O5 = 1.942(3) Å for $Tp^*WO(PP)_2$] are typical of W−O single bonds; the W−O−C angles are 135.4(3)° and 135.5(3)° [142.0(5)° and 136.4(5)°], respectively. The tungsten atom lies 0.2655 Å [0.257 Å] out of the N_2O_2 equatorial plane toward the oxo ligand, and the O1−W−O angles are consequently opened to ca. 103°. The W−O1 vector is canted 107.6° [107.8°] away from the WO_2 plane and this is ascribed to repulsion between the π-bonding orbitals of the W≡O unit and the out-of-plane π orbitals of the phenolate oxygen atoms. The W−N*n*1 distances are dictated by the relative trans influence of the coligands, the W−N11 distance being lengthened by 0.164(4) Å [0.145(4) Å] relative to the other W−N bonds. The dihedral angle between the mean planes of the two phenyl groups in $Tp^*W(OPh)_2$ is 59°, with one resting in a cleft between pyrazolyl groups and the other directed away from the Tp* ligand. This suggests that steric effects do not participate in the orientation of these ligands, and the molecule possesses C_1 symmetry by virtue of this arrangement.

There are two very similar molecules in the asymmetric unit of $Tp^*WO(SPh)_2 \cdot {}^1/_2C_4H_8O$; we shall restrict our discussion to the structural parameters of molecule 1. The W−O1 distance of 1.698(7) Å and the W−S distances of 2.380(2) and 2.389(2) Å are typical of terminal oxo and thiophenolate ligands on tungsten. As with $Tp^*WO(OPh)_2$ and $Tp^*WO(PP)_2$ (vide supra), the O1−W−S angles are ∼100° and the O1−W−N11 angle is 172.2(3)°. The W−S−C angles are 116.4(3)° and 113.0(3)°, significantly smaller than those of the phenolate complexes above, in accordance with other molybdenum and tungsten thiolate structures.[13,26,52] The W−O1 bond is canted 103.6°

dx.doi.org/10.1021/ic200161m |*Inorg. Chem.* 2011, 50, 4503–4514

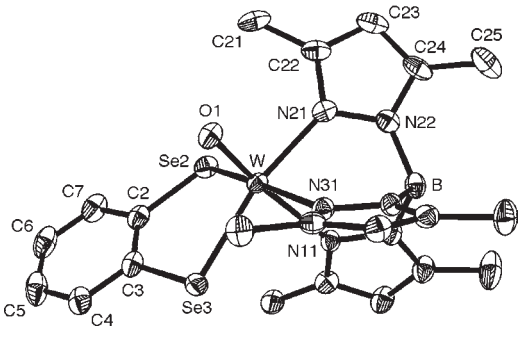

Figure 4. ORTEP projection and partial labeling scheme for Tp*WO(bds).

Table 4. Isotropic and Anisotropic Spin Hamiltonian Parameters for Tp*WOXY Complexes

compound	g_1	g_2	g_3	$\langle g\rangle^a$	g_{iso}	anisotropy[b]	A_{iso}[c]
Tp^*WOCl_2	1.8441	1.7994	1.7679	1.8038	1.8017	0.0762	81
Tp*WO(OPh)Cl	1.8448	1.8064	1.7258	1.7923	1.7882	0.1190	83
$Tp^*WO(OPh)_2$	1.8469	1.8022	1.7072	1.7854	1.7741	0.1397	85
$Tp^*WO(PP)_2$	1.8434	1.7956	1.7020	1.7821	1.7779	0.1414	86
Tp*WO(SPh)Cl	1.9025	1.8331	1.7767	1.8374	1.8359	0.1258	76
$Tp^*WO(SPh)_2$	1.9466	1.8429	1.8054	1.8650	1.8663	0.1412	60
Tp*WO(tdt)	1.9539	1.8857	1.8022	1.8806	1.8919	0.1517	57
Tp*WO(qdt)	1.9563	1.8927	1.8294	1.8920	1.8933	0.1541	61
$Tp^*WO(SePh)_2$	2.0084	1.8322	1.8083	1.8829	1.8832	0.2001	60
Tp*WO(bds)	1.9965	1.8994	1.8224	1.9061	1.9010	0.1741	56
Tp^*WOI_2	2.0412	1.8278	1.7587	1.8759	1.8778	0.2825	90[d]

[a] $\langle g\rangle = {}^1/_3(g_1 + g_2 + g_3)$; g_i values are taken directly from the experimental spectrum. [b] Anisotropy, $\Delta g = g_1 - g_3$. [c] Obtained by the simulation of isotropic spectra using *Simfonia* ($\times 10^{-4}$ cm^{-1}). [d] There is an unresolved ^{127}I ($I = {}^5/_2$, 100% abundance) superhyperfine contribution to the linewidth that has not been accounted for in the simulation.

away from the WS_2 plane. The least-squares planes of the two phenyl rings confer a dihedral angle of 49.2° with respect to each other. The S···S intramolecular distance of 3.403 Å is at the limit of the van der Waals contact distance for such an interaction (3.47 Å). The trans influence of the oxo ligand is manifest in a lengthening of the W−N11 bond by ca. 0.16 Å compared to the other W−N bonds. The complex exhibits a structure very similar to that reported for $Tp^*MoO(SPh)_2$.[13]

The crystal structure of the hexane hemisolvate of Tp*WO(bds) is the first one reported for an oxotungsten complex with a diselenolene ligand. Selected bond lengths and angles are listed in Table 3; an ORTEP projection is shown in Figure 4. The W−O1 distance of 1.704(3) Å associated with the terminal oxo ligand is within expectations. The W−Se2 and W−Se3 distances are 2.5143(5) and 2.5038(5) Å, respectively, and the associated W−Se−C angles are 100.9(1)° and 101.0(1)°. The W−Se and Se−C distances are slightly longer, and the W−Se−C angles are ca. 7° smaller for Tp*WO(bds) than those reported for $W(CO)_2(bds)_2$.[53] The Se−W−Se chelate bite angle of 86.70(1)° is ca. 3° larger than that for $W(CO)_2(bds)_2$. The tungsten atom lies 0.25 Å above the equatorial plane defined by Se2, Se3, N21, and N31 toward the oxo ligand. The W−N11 distance is lengthened by ca. 0.21 Å relative to the other two W−N bonds. This trans influence is marginally smaller than that in the molybdenum analogue, Tp*MoO(bds),[54] with an otherwise near-identical structure. The aromatic C−C bond lengths are all

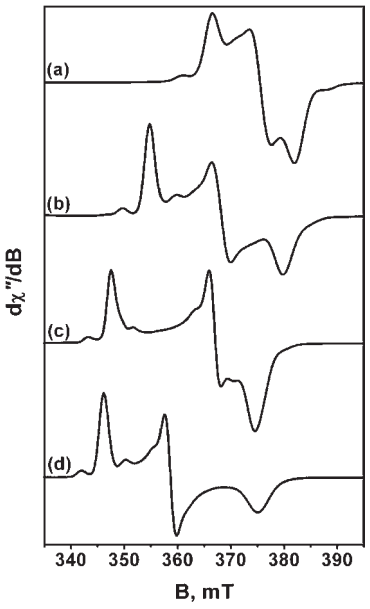

Figure 5. Frozen-glass X-band EPR spectra revealing the effect on the **g** tensor in the series (a) Tp^*WOCl_2, (b) Tp*WO(SPh)Cl, (c) $Tp^*WO(SPh)_2$, and (d) Tp*WO(tdt).

equivalent, as are the W−Se and Se−C distances, such that bds^{2-} can be described as a dianionic ligand, possessing no π-radical character.[55] The fold angle, defined as the dihedral angle between the W−Se2−Se3 and Se2−Se3−C2−C3 planes, is 24.8°. The molybdenum analogue has a slightly larger fold angle of 26.1°.[54] It is expected that selenium closely mimics the properties of sulfur in small inorganic models of enzyme active sites; however, because of the dearth of relevant crystal structures, there has been no systematic analysis of the fold angles in Mo/W−S versus Mo/W−Se complexes.

EPR Spectroscopy. Fluid-solution EPR spectra were recorded in THF or dichloromethane, while frozen-glass spectra were recorded using THF/*N*,*N*-dimethylformamide (DMF) or dichloromethane/DMF glasses. The anisotropic *g* values obtained directly from the experimental low-temperature spectra and isotropic *g* and *A* values from spectral simulations are presented in Table 4. Isotropic X-band EPR spectra were typical of a single oxotungsten(V) d^1 center, with g_{iso} significantly lower than that of the free-electron ($g_e = 2.0023$) because of the large spin−orbit coupling constant for tungsten ($\zeta_W = 2700$ cm^{-1}).[56] Hyperfine features due to ^{183}W ($I = {}^1/_2$; 14.31% natural abundance) were only discernible as shoulders on the main signal; thus, isotropic spectra were simulated to estimate the ^{183}W hyperfine coupling constant. Low g_{iso} and large A_{iso} parameters typify these tungstenyl complexes, and the observed correlation follows the trend identified with the molybdenyl series (Figure S1 in the Supporting Information).[13]

A highly anisotropic spectrum is observed at low temperatures, where only the tungsten hyperfine associated with g_1 is clearly visible in all samples. The anisotropy increases in going from the Cl^- and monodentate SPh^- complexes to the bidentate tdt^{2-} complex (Figure 5). The presence of a metallodithiolene in the latter increases the covalency, and the higher *g* values are ascribed to an increase in the ground-to-excited-state transitions as a result of pπ−dπ interactions in this compound.[12,57] The electronic absorption spectra for Tp*WO(tdt) and Tp*WO(qdt) clearly

dx.doi.org/10.1021/ic200161m |*Inorg. Chem.* 2011, 50, 4503–4514

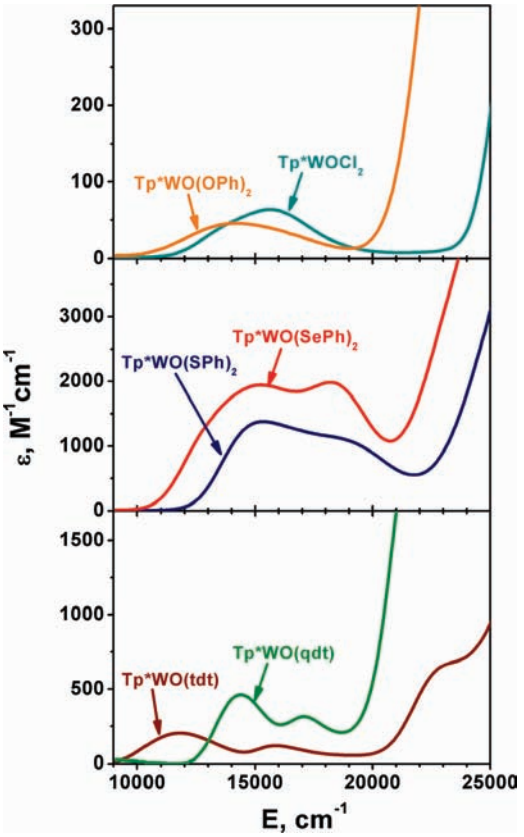

Figure 6. Overlay of the electronic spectra of top: Tp^*WOCl_2 and $Tp^*WO(OPh)_2$, middle: $Tp^*WO(SPh)_2$ and $Tp^*WO(SePh)_2$, and bottom: Tp*WO(tdt) and Tp*WO(qdt). All spectra were recorded in dichloromethane at room temperature.

show low-energy ligand-to-metal charge-transfer (LMCT) bands that contribute to an increase in the **g** tensor.[58]

Only Tp^*WOI_2 and $Tp^*WO(SePh)_2$ have $g_1 > g_e$, a result solely due to the large spin−orbit coupling constants for iodine and selenium.[59] The presence of weakly covalent W−I bonds is consistent with the large ^{183}W hyperfine coupling constant and weak intensity of the purported low-energy LMCT bands (Figure S3 in the Supporting Information). Moreover, the g_2 and g_3 values are quite similar for $Tp^*WO(SPh)_2$ and $Tp^*WO(SePh)_2$, showing that there is little disruption in the ligand-field (LF) splitting when sulfur is substituted by selenium (Figure S2 in the Supporting Information). The low isotopic abundance of ^{77}Se ($I = {}^1/_2$; 7.58% natural abundance) and inherently broad line shapes masked any ligand superhyperfine features in the spectra of $Tp^*WO(SePh)_2$ and Tp*WO(bds). Such nuclear interactions were not observed in (L3S)MoO$(SePh)_2$ [L3S = (2-dimethylethanethiol)bis(3,5-dimethylpyrazol-1-yl)methane][60] and were only revealed at S-band frequencies for $NEt_4[MoO(SePh)_4]$ and $NEt_4[WO(SePh)_4]$.[61] These compounds are currently the subject of a multifrequency EPR study that will be the focus of a separate publication.

Electronic Absorption Spectroscopy. The electronic absorption spectra of the Tp*WOXY complexes can be classified into two categories. Where X and Y are hard donor ligands (O, Cl), a LF transition at ∼15 000 cm^{-1} ($\varepsilon > 100\ M^{-1}\ cm^{-1}$) is the only feature in the low-energy region, below 25 000 cm^{-1} (Figure 6, top). For soft donors (S, Se), this formally forbidden transition is obscured by low-energy LMCT bands because the 3p and 4p orbitals are energetically closer to the W d manifold (Figure 6, middle). Such LF transitions have been found in the range of 13 000−16 000 cm^{-1} in other mononuclear tungstenyl complexes[22] and defined as a transition from the singularly occupied W $d_{x^2-y^2}$ ground-state orbital (SOMO) to W d_{xz}/d_{yz} π^* orbitals.

Scheme 2. Two Nearly Isoenergetic Tautomeric Forms of $qdtH_2$ and qdt^{2-}

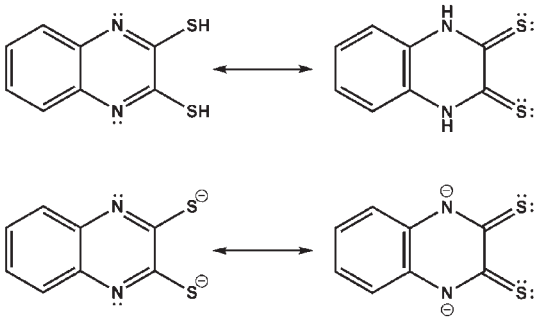

The spectrum of Tp^*WOI_2 exhibits two low-energy features lacking any appreciable charge-transfer (CT) intensity ($\varepsilon < 90\ M^{-1}\ cm^{-1}$; Figure S3 in the Supporting Information). It is possible that these weak bands infer a lifting of the degeneracy of the d_{xz}/d_{yz} π^* orbital. However, with a strong-field axial ligand, this scenario is implausible, and the absorption peak at 13 200 cm^{-1} is assigned as a weak LMCT band. The band at 15 015 cm^{-1} may be described as a LF transition. The spectral features of $Tp^*WO(SPh)_2$ and $Tp^*WO(SePh)_2$ are very similar, with two absorption bands at low energy (15 400 and 17 900 cm^{-1} for $Tp^*WO(SPh)_2$; 15 200 and 18 200 cm^{-1} for $Tp^*WO(SePh)_2$) assigned to S/Se → W $d_{x^2-y^2}$ transitions (Figure 6, middle). The lowest peak is slightly red-shifted for $Tp^*WO(SePh)_2$, and the intensity of the band, as was expected for the larger chalcogen, is considerably enhanced. The same trend is apparent when comparing Tp*WO(tdt) and Tp*WO(bds) and has been previously noted for $NEt_4[MO(EAr)_4]$ (M = Mo, W; E = S, Se).[29,60]

The complexes Tp*WO(tdt) and Tp*WO(qdt) (Figure 6, bottom) have only two low-energy features compared to the three distinct features below ∼20 000 cm^{-1} for the analogous molybdenum compounds.[20,62] Rigorous spectroscopic studies of the molybdenum series classified two lowest bands as LMCT transitions from out-of-plane S p orbitals to the $d_{x^2-y^2}$ ground state.[20] Absorption bands shifted ∼3000 cm^{-1} to higher energy when tungsten was substituted for molybdenum, consistent with previous observations,[20] and the electron-withdrawing nature of the quinoxaline group effects a further blue shift of these bands. The qdt^{2-} ligand has two nearly isoenergetic resonance structures (Scheme 2) that attenuate its π-donating capability,[17] though interestingly, these bands are more intense than those for Tp*WO(tdt). The opposite condition was shown for the molybdenum analogues and may indicate a larger dithiolene fold angle in the tungsten complexes, thus increasing the orbital overlap between the out-of-plane S p orbitals and the W $d_{x^2-y^2}$ orbital. A magnetic circular dichroism (MCD) study of these compounds is currently underway and aims to unambiguously assign these bands. The intense feature at 26 500 cm^{-1}, absent in

dx.doi.org/10.1021/ic200161m |*Inorg. Chem.* 2011, 50, 4503–4514

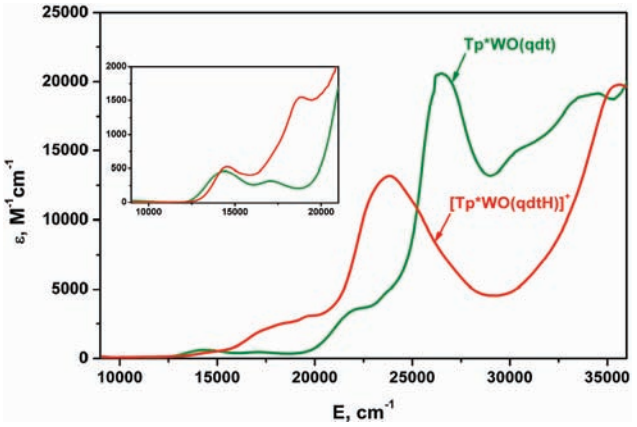

Figure 7. Effect of acid on the electronic absorption spectrum of Tp*WO(qdt) in dichloromethane. The neutral complex is shown in green and the protonated species in red. Inset: magnification of the low-energy region.

Tp*WO(tdt), is a feature of oxidized quinoxalines and pterins[63] and was assigned as a quinoxaline $\pi \rightarrow \pi^*$ transition in Tp*MoO(qdt).[18]

The treatment of Tp*WO(qdt) with 1 equiv of trifluoroacetic acid (TFA) produced a dramatic color change from green to red-brown. Further equivalents of acid did not alter the resultant electronic absorption spectrum (Figure 7). These spectral features are fully reversible with the addition of base, in this instance pyridine, restoring the original spectrum. The first bands of both spectra have very similar energy and intensity, whereas the following band shows a substantial increase in the intensity and a blue shift of ~1500 cm^{-1} for the protonated species. We propose that one quinoxaline nitrogen atom has been protonated in a manner similar to the treatment of $(PPh_4)_2[Mo(qdt)_3]$ with acid.[64] A red shift of the quinoxaline $\pi \rightarrow \pi^*$ transition by 2500 cm^{-1} is consistent with previous observations of protonating $[Pt(qdt)_2]^{2-}$ [65,66] and other nitrogen-containing heterocyclic dithiolenes.[67] The presence of this transition shows that quinoxaline retains its aromaticity. Crystallographically characterized $Ni^{II}(qdtH)_2$,[68] where $qdtH^-$ represents a monoprotonated qdt^{2-} ligand, shows only a slight lengthening of the bonds about the protonated nitrogen, while the ligand remains planar. The isotropic EPR spectra of $[Tp^*WO(qdtH)]^+$ shows a small decrease in g value compared to Tp*WO(qdt) (1.890 cf. 1.915, see Figure S4 in the Supporting Information), indicative of a slight increase in Z_{eff}. This is consistent with the formation of a weaker π-donating ligand and a concomitant positive shift of the reduction potential (vide infra). Also, the lower isotropic g value reflects a reduced LF splitting, with g_3 experiencing a noticeable shift to higher field (Figure S5 in the Supporting Information). Most interestingly, the isotropic tungsten hyperfine coupling constant is reduced to 43×10^{-4} cm^{-1} [from 61×10^{-4} cm^{-1} for Tp*WO(qdt)]; this is counterintuitive given the increase in Z_{eff} and suggests that the protonated system is more covalent. The π-donor capability of the qdt^{2-} ligand is greatly reduced upon protonation; however, σ donation may be enhanced. The increased covalency could result from a strengthening of the pseudo-σ bond, proposed by Kirk et al.[20] as the possible mechanism by which electrons are transported in pyranopterin-containing enzymes. Alternatively, the dithiolene fold angle could increase, along with the overlap between the out-of-plane

Table 5. Electrochemical Data

	tungsten(V/IV)			tungsten(VI/V)		
compound	$E_{1/2}$[a]	ΔE_{pp}[a]	I_{pa}/I_{pc}	$E_{1/2}$[a]	ΔE_{pp}[a]	I_{pa}/I_{pc}
Tp^*WOCl_2	−899	69	0.98	1205	73	1.60
Tp^*WOI_2	−598	72	0.86	1146	71	1.32
$Tp^*WO(OPh)_2$	−1464	66	1.02	202	65	0.97
$Tp^*WO(PP)_2$	−1514	59	0.96	207	90	1.00
Tp*WO(SPh)Cl	−811	70	0.86	715	69	1.13
$Tp^*WO(SPh)_2$	−622	61	0.86	568	69	1.03
Tp*WO(tdt)[b]	−569	75	0.97	708	94	1.14
Tp*WO(qdt)[b]	−406	72	1.04	1180		
$Tp^*WO(SePh)_2$	−667	69	0.87	422	66	1.03
Tp*WO(bds)	−441	73	0.84	809		

[a] Potentials in millivolts ($E_{1/2}$ versus SCE). [b] Recorded in dichloromethane (others in acetonitrile).

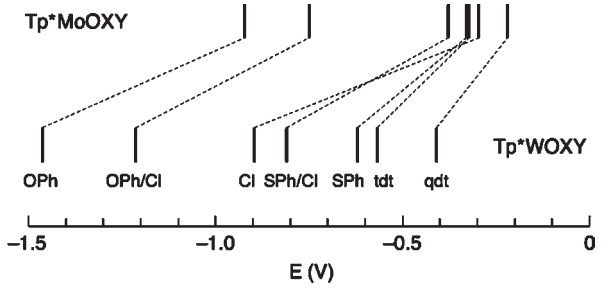

Figure 8. Comparison of the $Mo^{V/IV}$ reduction potentials for Tp*MOXY complexes (M = Mo, W; X = Y as specified, unless indicated). The vertical bars represent the potentials of the specified derivatives versus SCE. Data for molybdenum compounds were taken from refs 13, 18 and 33.

S 3p orbitals and the W $d_{x^2-y^2}$, orbital; this would decrease the antibonding interaction between these sulfur orbitals and the W≡O π^* orbitals ($d_{xz,yz}$), and afford a smaller LF splitting while maintaining the covalency.

Electrochemistry. Cyclic voltammograms were recorded for all Tp*WOXY complexes, and the data presented in Table 5 fall into two groups. All oxotungsten(V) complexes with monodentate ligands possess two quasi-reversible processes, as shown by the I_{pa}/I_{pc} value of about unity (Figure S6 in the Supporting Information). The cathodic process is defined as a one-electron reduction from W^V to W^{IV} and the quasi-reversible anodic process as a one-electron oxidation to W^{VI}. The ΔE_{pp} values of ~ 59 mV are in accordance with a one-electron process, and this was confirmed by controlled-potential coulometry of the analogous molybdenum compound, $Tp^*MoO(SPh)_2$ (0.96 electrons/Mo).[13] The reduction potentials span a range of ~1.1 V, with the bis(phenolate) compounds the most difficult to reduce, and show that the redox potentials are dictated by the electronic nature of the X, Y ligand. The highly covalent thiolate and selenolate complexes display more facile reduction of the metal ion than their oxygen counterparts. The trend in the reduction potentials resembles that of the molybdenum series,[13,69] with W(V) being 200−600 mV more difficult to reduce than Mo(V) (Figure 8). As such, they can be defined as essentially metal-based rather than ligand-based redox processes, though there is

dx.doi.org/10.1021/ic200161m |Inorg. Chem. 2011, 50, 4503–4514

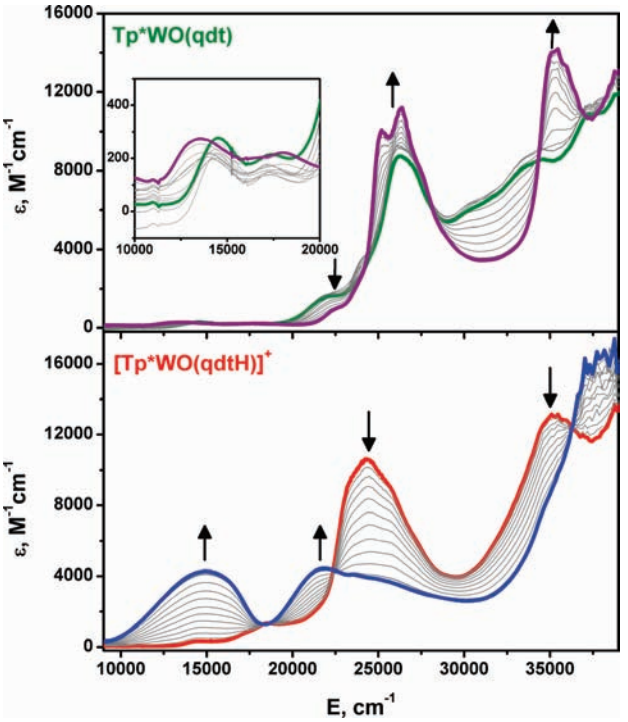

Figure 9. Top: Electronic absorption spectra of Tp*WO(qdt) (green) and its coulometrically generated one-electron-reduced form, $[Tp^*WO(qdt)]^-$ (purple), in dichloromethane containing 0.20 M $N^nBu_4PF_6$ as the supporting electrolyte at −20 °C. Bottom: Electronic absorption spectra of $[Tp^*WO(qdtH)]^+$ (red) and its coulometrically generated one-electron-reduced form (blue) in dichloromethane containing 0.2 M $N^nBu_4PF_6$ and an excess of TFA at −20 °C.

substantial ligand character in the ground-state SOMO.[62,70] Such contrasts have been seen before with tungsten(IV,V,VI) complexes when compared to molybdenum analogues.[71,72] The difference diminishes with S- and Se-donor ligands. Substituting selenium for sulfur does not greatly perturb the reduction potential[72] and highlights the similar electronic structures of the thiolate and selenolate complexes.

The bidentate complexes Tp*WO(tdt) and Tp*WO(qdt) have even more facile reduction processes than $Tp^*WO(SPh)_2$, with $W^{V/IV}$ potentials of −569 and −406 mV for Tp*WO(tdt) and Tp*WO(qdt), respectively. Controlled-potential coulometry on Tp*WO(qdt) at −20 °C confirmed this reduction to be reversible. The electronic absorption spectrum of the reduced product revealed that the quinoxaline $\pi \rightarrow \pi^*$ transition is retained, although it manifests as two peaks separated by 1000 cm^{-1} (Figure 9, top). Similar findings have been reported for mono- and bis(quinoxalinedithiolate) complexes of platinum.[73] Interestingly, there is no apparent change in the low-energy region of the spectrum (inset, Figure 9, top), with the energy and intensity of the purported out-of-plane S 3p → W $d_{x^2-y^2}$ LMCT transitions being similar in both spectra despite the reduced product having a formal W^{IV} $(d_{x^2-y^2})^2$ configuration. It appears that simply transferring the band assignments of Tp*MoO(qdt) to this tungsten analogue is not valid and that the corresponding transition in Tp*WO(qdt) may shift to energies below 9000 cm^{-1} (outside the detectable region). This underscores the difficulty in unambiguously assigning the overlapping bands in the electronic absorption spectra of molybdenum and tungsten monodithiolene complexes without more advanced spectroscopic measurements.

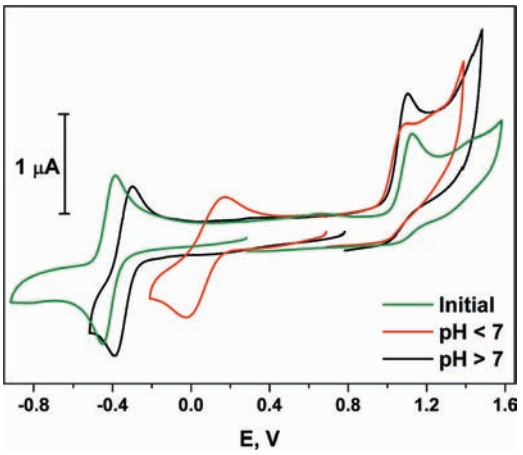

Figure 10. Cyclic voltammogram of $Tp^*WO(qdt)_2$ in dichloromethane containing $N^nBu_4PF_6$ (0.2 M) as the supporting electrolyte at ambient temperature (green trace). The voltammogram after treatment with excess acid (red trace) and the initial voltammogram after the addition of an equal amount of pyridine (black trace), both recorded at −20 °C. Scans were conducted at a rate of 100 mV s^{-1} and potentials referenced to SCE.

The cathodic (oxidation) process of Tp*WO(tdt) is quasi-reversible in dichloromethane and irreversible in acetonitrile. For Tp*WO(qdt), the quasi-reversible oxidation is ∼380 mV more positive than it is for its molybdenum analogue. This underscores tungsten's preference for higher oxidation states and supports the observed formation of colorless dioxotungsten(VI) species upon aerial oxidation of these Tp*WOXY compounds. The electron-withdrawing nature of qdt^{2-} makes the reduction potential significantly more positive compared to tdt^{2-}. This is attributed to the removal of the charge density away from the dithiolene sulfur atoms with a concomitant increase in Z_{eff} on the tungsten ion (Scheme 2).

The redox chemistry of Tp*WO(tdt) and Tp*WO(qdt) was investigated in protic media. As was observed by electronic absorption spectroscopy, green Tp*WO(qdt) became red-brown upon protonation. The voltammograms of protonated and deprotonated Tp*WO(qdt) (Figure 10) were recorded using an excess of acid and base (∼3 equiv) at −20 °C. As expected, the protonated ligand, $qdtH^-$, is considerably more electron-withdrawing, as is illustrated by the positive shift of the reduction potential to +74 mV. This process is irreversible at room temperature. Although ΔE_{pp} increases to 202 mV, the process is reversible by coulometry. The same non-Nernstian behavior is seen in the voltammogram of Tp*WO(tdt) (ΔE_{pp} = 240 mV) in the presence of 2 equiv of TFA (Figure S7 in the Supporting Information). This may indicate weak interactions of the proton-rich electrolyte with the terminal oxo ligand. There was no pronounced shift in the reduction potential for Tp*WO-(tdt), which confirms that acid only interacts with the qdt^{2-} ligand. The addition of base led to the reappearance of the original green color of the Tp*WO(qdt) solution, and the reduction potential was almost fully restored [albeit with a +60 mV shift, which we attribute to the altered electrolyte medium; Tp*WO(tdt) also exhibited a similar small positive shift], demonstrating that this complex is reversibly protonated and reduced.

dx.doi.org/10.1021/ic200161m |*Inorg. Chem.* 2011, 50, 4503–4514

Scheme 3. Principal Canonical Forms of $[Tp^*WO(qdtH_2)]^+$

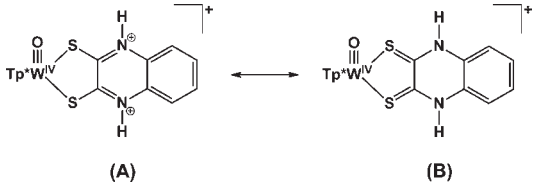

The electronic absorption spectrum of reduced $[Tp^*WO(qdtH)]^+$ shows clean isosbestic points at 18 490, 22 370, and 36 230 cm^{-1}, indicating the presence of only two absorbing species in solution (Figure 9, bottom). However, there are some profound differences, particularly the absence of the prominent qdt^{2-} $\pi \rightarrow \pi^*$ transition at ~24 300 cm^{-1} and the generation of a very intense band at 14 900 cm^{-1}. This latter transition has >10 times the intensity of the lowest-energy CT band in $Tp^*WO(qdt)$. This unique spectrum may arise from an increase in the ligand basicity upon reduction, leading to protonation of the second nitrogen. If we consider the two resonance structures in Scheme 3, adapted from those depicted for $qdtH_2$ (Scheme 2), we suggest that the loss in intensity of the $\pi \rightarrow \pi^*$ transition stems from a substantial contribution from canonical form B to the electronic structure of the complex. This may also be responsible for the intense near-IR (NIR) transition (ε = 4400 M^{-1} cm^{-1}), which may be either a LMCT band or an intraligand transition within this neutral dithione moiety. A deeper understanding of the distinctive property features exhibited by these complexes will require additional spectroscopic measurements.

CONCLUSIONS

The preparation of a series of tungstenyl complexes of the general formula Tp*WOXY has been achieved via metathesis of the dihalo precursors, Tp^*WOCl_2 and Tp^*WOI_2, with ligand salts. This has facilitated spectroscopic characterization of the $\{W{\equiv}O\}^{3+}$ moiety and a comparison with the molybdenyl analogues. The d^1 tungsten(V) complexes exhibit various colors, exemplified by sky-blue Tp^*WOCl_2, grass-green $Tp^*WO(OPh)_2$, dark-red Tp^*WOI_2, and the intense blue and green of $Tp^*WO(SPh)_2$ and $Tp^*WO(SePh)_2$, respectively. The electronic structure of the tungstenyl unit is very similar to that of the molybdenyl unit, with the same trends seen in EPR and electronic absorption spectra and cyclic voltammetry. Compounds with the heavier metal have lower g values because of the increased spin−orbit coupling of tungsten, shifts of 2000−3000 cm^{-1} in the electronic LF transitions, a reduction in the intensity of CT bands from S- and Se-donor ligands, and are ca. 400 mV more difficult to reduce than their molybdenum counterparts.

Aromatic dithiolate complexes, $Tp^*WO(tdt)$ and $Tp^*WO(qdt)$, represent the first oxotungsten(V) monodithiolene species that possess the minimum structural elements of tungstoenzymes and tungsten-substituted molybdoenyzmes. Electronic absorption spectroscopy and cyclic voltammetry have revealed a reversible reduction and protonation of the pyrazine nitrogen atoms of qdt^{2-}. The highly electron withdrawing ligand, $qdtH^-$, is formed and affects a substantial positive shift of the reduction potential. We propose that an increase in the ligand basicity upon reduction of $[Tp^*WO(qdtH)]^+$ promotes a second protonation of the quinoxaline group. The changes to the electronic absorption spectrum are quite profound, and we observe a very intense band in the NIR region at 15 000 cm^{-1}. Such a system may find application in chemical sensors.

This series of tungstenyl complexes is now available for further studies employing advanced spectroscopic techniques, namely, multifrequency EPR, MCD, and X-ray absorption spectroscopies, that will elucidate the electronic structure of this biologically and industrially important $\{W{\equiv}O\}^{3+}$ moiety.

ASSOCIATED CONTENT

Supporting Information. X-ray crystallographic files in CIF format, electronic absorption spectrum of Tp^*WOI_2, X-band EPR spectra of $Tp^*WO(EPh)_2$ (E = O, S, Se), room temperature and low-temperature EPR spectra of Tp*WO(qdt) and $[Tp^*WO(qdtH)]^+$, correlation plot of g_{iso} vs A_{iso} for the complexes, and cyclic voltammograms of $Tp^*WO(SPh)_2$ and Tp*WO(tdt) in acid and base. This material is available free of charge via the Internet at http://pubs.acs.org.

AUTHOR INFORMATION

Corresponding Author

*E-mail: sproules@mpi-muelheim.mpg.de (S.S.), cgyoung@unimelb.edu.au (C.G.Y.).

Present Address

‡School of Science and Technology, University of New England, Armidale, New South Wales 2351, Australia.

ACKNOWLEDGMENT

We thank Jason Hill for preliminary syntheses and Sioe See Volaric for mass spectrometric measurements. We are indebted to Dr. Eberhard Bothe and Petra Höfer of the Max-Planck-Institut für Bioanorganische Chemie for spectroelectrochemical measurements. Financial support from the Australian Research Council is gratefully acknowledged.

REFERENCES

(1) Hough, D. W.; Danson, M. J. *Curr. Opin. Chem. Biol.* **1999**, *3*, 39.
(2) Davies, P. W. C. *The Fifth Miracle: The Search for the Origin and Meaning of Life*; Simon & Schuster: New York, 1999.
(3) Andreesen, J. R.; Makdessi, K. *Ann. N.Y. Acad. Sci.* **2008**, *1125*, 215.
(4) (a) Mukund, S.; Adams, M. W. W. *J. Biol. Chem.* **1991**, *266*, 14208. (b) Mukund, S.; Adams, M. W. W. *J. Biol. Chem.* **1995**, *270*, 8389. (c) Roy, R.; Mukund, S.; Schut, G. J.; Dunn, D. M.; Weiss, R.; Adams, M. W. W. *J. Bacteriol.* **1999**, *181*, 1171. (d) Roy, R.; Adams, M. W. W. *J. Bacteriol.* **2002**, *184*, 6952. (e) Bevers, L. E.; Bol, E.; Hagedoorn, P.-L.; Hagen, W. R. *J. Bacteriol.* **2005**, *187*, 7056.
(5) Stiefel, E. I. *Molybdenum Enzymes, Cofactors and Model Systems*; American Chemical Society: Washington, DC, 1993; Vol. 535.
(6) (a) Hille, R. *Chem. Rev.* **1996**, *96*, 2757. (b) Johnson, M. K.; Rees, D. C.; Adams, M. W. W. *Chem. Rev.* **1996**, *96*, 2817.
(7) Bevers, L. E.; Hagedoorn, P.-L.; Hagen, W. R. *Coord. Chem. Rev.* **2009**, *253*, 269.
(8) Romão, M. J. *Dalton Trans.* **2009**, 4053.
(9) (a) Boll, M.; Schink, B.; Messerschmidt, A.; Kroneck, P. M. H. *Biol. Chem.* **2005**, *386*, 999. (b) Chan, M. K.; Mukund, S.; Kletzin, A.; Adams, M. W. W.; Rees, D. C. *Science* **1995**, *267*, 1463. (c) Raaijmakers, H.; Maceira, S.; Dias, J. M.; Teixeira, S.; Bursakov, S.; Huber, R.; Moura, J. J. G.; Moura, I.; Romão, M. J. *Structure* **2002**, *10*, 1261. (d) Seiffert, G. B.; Ullmann, G. M.; Messerschmidt, A.; Schink, B.; Kroneck, P. M. H.; Einsle, O. *Proc. Natl. Acad. Sci. U.S.A.* **2007**, *104*, 3073. (e) Stewart, L. J.;

Bailey, S.; Bennett, B.; Charnock, J. M.; Garner, C. D.; McAlpine, A. S. *J. Mol. Biol.* **2000**, *299*, 593.
(10) Hille, R. *Trends Biochem. Sci.* **2002**, *37*, 360.
(11) (a) Sugimoto, H.; Tsukube, H. *Chem. Soc. Rev.* **2008**, *37*, 2609. (b) Young, C. G.; Wedd, A. G. *Chem. Commun.* **1997**, 1251. (c) Enemark, J. H.; Cooney, J. J. A.; Wang, J.-J.; Holm, R. H. *Chem. Rev.* **2004**, *104*, 1175.
(12) Chang, C. J. S.; Collison, D.; Mabbs, F. E.; Enemark, J. H. *Inorg. Chem.* **1990**, *29*, 2261.
(13) Cleland, W. E., Jr.; Barnhart, K. M.; Yamanouchi, K.; Collison, D.; Mabbs, F. E.; Ortega, R. B.; Enemark, J. H. *Inorg. Chem.* **1987**, *26*, 1017.
(14) (a) Graff, J. N.; McElhaney, A. E.; Basu, P.; Gruhn, N. E.; Chang, C.-S.; Enemark, J. H. *Inorg. Chem.* **2002**, *41*, 2642. (b) Inscore, F. E.; Joshi, H. K.; McElhaney, A. E.; Enemark, J. H. *Inorg. Chim. Acta* **2002**, *331*, 246.
(15) Dhawan, I. K.; Enemark, J. H. *Inorg. Chem.* **1996**, *35*, 4873.
(16) Dhawan, I. K.; Pacheco, A.; Enemark, J. H. *J. Am. Chem. Soc.* **1994**, *116*, 7911.
(17) Helton, M. E.; Gruhn, N. E.; McNaughton, R. L.; Kirk, M. L. *Inorg. Chem.* **2000**, *39*, 2273.
(18) Helton, M. E.; Kirk, M. L. *Inorg. Chem.* **1999**, *38*, 4384.
(19) Inscore, F. E.; Knottenbelt, S. Z.; Rubie, N. D.; Joshi, H. K.; Kirk, M. L.; Enemark, J. H. *Inorg. Chem.* **2006**, *45*, 967.
(20) Inscore, F. E.; McNaughton, R. L.; Westcott, B. L.; Helton, M. E.; Jones, R.; Dhawan, I. K.; Enemark, J. H.; Kirk, M. L. *Inorg. Chem.* **1999**, *38*, 1401.
(21) Okamura, T.; Ueyama, N. In *Comprehensive Coordination Chemistry II*; McCleverty, J. A., Meyer, T. J., Eds.; Elsevier: New York, 2003; Vol. 4, pp 529−573.
(22) (a) Crouch, P. C.; Fowles, G. W. A.; Marshall, P. R.; Walton, R. A. *J. Chem. Soc. A* **1968**, 1634. (b) Levason, W.; McAuliffe, C. A.; McCullough, F. P. J. *Inorg. Chem.* **1977**, *16*, 2911.
(23) (a) Fowles, G. W. A.; Frost, J. L. *J. Chem. Soc. A* **1967**, 671. (b) Hornung, F. R.; Kaim, W. *J. Chem. Soc., Faraday Trans.* **1994**, *90*, 2909. (c) Levason, W.; McAuliffe, C. A.; McCullough, F. P. *Inorg. Chim. Acta* **1977**, *24*, L13. (d) Levason, W.; McAuliffe, C. A.; McCullough, F. P.; Murray, S. G.; Rice, C. A. *Inorg. Chim. Acta* **1977**, *22*, 227. (e) Levason, W.; McCullough, F. P. J.; McAuliffe, C. A. *Inorg. Nucl. Chem. Lett.* **1976**, *12*, 843.
(24) Rice, C. A.; Kroneck, P. M. H.; Spence, J. T. *Inorg. Chem.* **1981**, *20*, 1996.
(25) (a) Das, S. K.; Biswas, D.; Maiti, R.; Sarkar, S. *J. Am. Chem. Soc.* **1996**, *118*, 1387. (b) Davies, E. S.; Aston, G. R.; Beddoes, R. L.; Collison, D.; Dinsmore, A.; Docrat, A.; Joule, J. A.; Wilson, C. R.; Garner, C. D. *J. Chem. Soc., Dalton Trans.* **1998**, 3674. (c) Goddard, C. A.; Holm, R. H. *Inorg. Chem.* **1999**, *38*, 5389.
(26) Sung, K.-M.; Holm, R. H. *Inorg. Chem.* **2001**, *40*, 4518.
(27) (a) Baba, K.; Okamura, T.; Yamamoto, H.; Yamamoto, T.; Ohama, M.; Ueyama, N. *Inorg. Chem.* **1996**, *45*, 8365. (b) Oku, H.; Ueyama, N.; Nakamura, A. *Chem. Lett.* **1995**, 621.
(28) (a) Lorber, C.; Donahue, J. P.; Goddard, C. A.; Nordlander, E.; Holm, R. H. *J. Am. Chem. Soc.* **1998**, *120*, 8102. (b) Ueyama, N.; Oku, H.; Nakamura, A. *J. Am. Chem. Soc.* **1992**, *114*, 7310.
(29) Hanson, G. R.; Brunette, A. A.; McDonell, A. C.; Murray, K. S.; Wedd, A. G. *J. Am. Chem. Soc.* **1981**, *103*, 1953.
(30) Ellis, S. R.; Collison, D.; Garner, C. D.; Clegg, W. *Chem. Commun.* **1986**, 1483.
(31) (a) Fleischer, E. B.; Chapman, R. D.; Krishnamurthy, M. *Inorg. Chem.* **1979**, *18*, 2156. (b) Krishnamurthy, M. *Inorg. Chim. Acta* **1979**, *32*, L32.
(32) Laye, R. H.; Bell, Z. R.; Ward, M. D. *New J. Chem.* **2003**, *27*, 684.
(33) Stobie, K. M.; Bell, Z. R.; Munhoven, T. W.; Maher, J. P.; McCleverty, J. A.; Ward, M. D.; McInnes, E. J. L.; Totti, F.; Gatteschi, D. *Dalton Trans.* **2003**, 36.
(34) McDonagh, A. M.; Ward, M. D.; McCleverty, J. A. *New J. Chem.* **2001**, *25*, 1236.
(35) Eagle, A. A.; Tiekink, E. R. T.; Young, C. G. *Inorg. Chem.* **1997**, *36*, 6315.
(36) Trofimenko, S. *J. Am. Chem. Soc.* **1969**, *91*, 588.
(37) Thomas, S.; Young, C. G. *Inorg. Synth.* **2002**, *33*, 218.
(38) Young, C. G.; Thomas, S.; Gable, R. W. *Inorg. Chem.* **1998**, *37*, 1299.
(39) Morrison, D. C.; Furst, A. *J. Org. Chem.* **1956**, *21*, 470.
(40) Sandman, D. J.; Allen, G. W.; Acampora, L. A.; Stark, J. C.; Jansen, S.; Jones, M. T.; Ashwell, G. J.; Foxman, B. M. *Inorg. Chem.* **1987**, *26*, 1664.
(41) *WINEPR Simfonia*; Bruker Analytische Messtechnik GmbH: Karlsruhe, Germany1996.
(42) Connelly, N. G.; Geiger, W. E. *Chem. Rev.* **1996**, *96*, 877.
(43) Thomas, S.; Young, C. G.; Tiekink, E. R. T. *Organometallics* **1998**, *17*, 182.
(44) Sheldrick, G. M. *Acta Crystallogr.* **2008**, *A64*, 112.
(45) Farrugia, L. J. *J. Appl. Crystallogr.* **1997**, *30*, 565.
(46) Farrugia, L. J. *J. Appl. Crystallogr.* **1999**, *32*, 837.
(47) van der Sluis, P.; Spek, A. L. *Acta Crystallogr.* **1990**, *A46*, 194.
(48) Barrado, G.; Doerrer, L.; Green, M. L. H.; Leech, M. A. *Dalton Trans.* **1999**, 1061 and references cited therein.
(49) Millar, M.; Lincoln, S.; Koch, S. A. *J. Am. Chem. Soc.* **1982**, *104*, 288.
(50) (a) Feng, S. G.; Luan, L.; White, P. S.; Brookhart, M. S.; Templeton, J. L.; Young, C. G. *Inorg. Chem.* **1991**, *30*, 2584. (b) Thomas, S.; Tiekink, E. R. T.; Young, C. G. *Inorg. Chem.* **2006**, *45*, 352.
(51) Kipke, C. A.; Cleland, W. E., Jr.; Roberts, S. A.; Enemark, J. H. *Acta Crystallogr.* **1989**, *C45*, 870.
(52) (a) Lim, B. S.; Holm, R. H. *J. Am. Chem. Soc.* **2001**, *123*, 1920. (b) Sung, K.-M.; Holm, R. H. *Inorg. Chem.* **2000**, *45*, 2979. (c) Xiao, Z.; Bruck, M. A.; Doyle, C.; Enemark, J. H.; Grittini, C.; Gable, R. W.; Wedd, A. G.; Young, C. G. *Inorg. Chem.* **1995**, *34*, 5950.
(53) Heckmann, G.; Wolmerhaeuser, G. *Chem. Ber.* **1993**, *126*, 1071.
(54) Williams, A.; Kirk, M. L. Personal communication.
(55) Herebian, D.; Bothe, E.; Bill, E.; Weyhermüller, T.; Wieghardt, K. *J. Am. Chem. Soc.* **2001**, *123*, 10012.
(56) Goodman, B. A.; Raynor, J. B. *Adv. Inorg. Chem. Radiochem.* **1970**, *13*, 135.
(57) Young, C. G.; Gable, R. W.; Hill, J. P.; George, G. N. *Eur. J. Inorg. Chem.* **2001**, 2227.
(58) (a) Balagopalakrishna, C.; Kimbrough, J. T.; Westmoreland, T. D. *Inorg. Chem.* **1996**, *35*, 7758. (b) Nipales, N. S.; Westmoreland, T. D. *Inorg. Chem.* **1997**, *36*, 756. (c) Swann, J.; Westmoreland, T. D. *Inorg. Chem.* **1997**, *36*, 5348.
(59) Mabbs, F. E.; Collison, D. *Electron Paramagnetic Resonance of d Transition Metal Compounds*; Elsevier: Amsterdam, The Netherlands, 1992.
(60) Peariso, K.; Chohan, B. S.; Carrano, C. J.; Kirk, M. L. *Inorg. Chem.* **2003**, *42*, 6194.
(61) Hanson, G. R.; Wilson, G. L.; Bailey, T. D.; Pilbrow, J. R.; Wedd, A. G. *J. Am. Chem. Soc.* **1987**, *109*, 2609.
(62) Kirk, M. L.; McNaughton, R. L.; Helton, M. E. *Prog. Inorg. Chem.* **2004**, *52*, 111.
(63) Gardlik, S.; Rajagopalan, K. V. *J. Biol. Chem.* **1991**, *266*, 4889.
(64) Boyde, S.; Garner, C. D. *J. Chem. Soc., Dalton Trans.* **1991**, 713.
(65) Cummings, S. D.; Eisenberg, R. *Inorg. Chem.* **1995**, *34*, 3396.
(66) Cummings, S. D.; Eisenberg, R. *Prog. Inorg. Chem.* **2004**, *52*, 491.
(67) Van Houten, K. A.; Walters, K. A.; Schanze, K. S.; Pilato, R. S. *J. Fluoresc.* **2000**, *10*, 35.
(68) Pignedoli, A.; Peyronel, G. *Acta Crystallogr.* **1977**, *B33*, 1439.
(69) McElhaney, A. E.; Inscore, F. E.; Schirlin, J. T.; Enemark, J. H. *Inorg. Chim. Acta* **2002**, *341*, 85.
(70) Drew, S. C.; Young, C. G.; Hanson, G. R. *Inorg. Chem.* **2007**, *46*, 2388.
(71) (a) Eagle, A. A.; Harben, S. M.; Tiekink, E. R. T.; Young, C. G. *J. Am. Chem. Soc.* **1994**, *116*, 9749. (b) Eagle, A. A.; Tiekink, E. R. T.; George, G. N.; Young, C. G. *Inorg. Chem.* **2001**, *40*, 4563. (c) Schulzke, C. *Dalton Trans.* **2005**, 713.
(72) Ma, X.; Starke, K.; Schulzke, C.; Schmidt, H.-G.; Noltemeyer, M. *Eur. J. Inorg. Chem.* **2006**, 628.
(73) Cummings, S. D.; Eisenberg, R. *Inorg. Chem.* **1995**, *34*, 2007.